Evidence for a Cr metastable phase as a tracer in DLI-MOCVD chromium hard coatings usable in high temperature environment

Alexandre Michau, Francis Maury, Frederic Schuster, Raphael Boichot, Michel Pons

Evidence for a Cr metastable phase as a tracer in DLI-MOCVD chromium hard coatings usable in high temperature environment

Alexandre Michau [a], Francis Maury [a,*], Frederic Schuster [b], Raphael Boichot [c], Michel Pons [c]

[a] CIRIMAT, CNRS/INPT/UPS, 4 allée E. Monso, 31030 Toulouse cedex 4, France
[b] CEA Saclay, DFP/DPg, 91191 Gif Sur Yvette, France
[c] University Grenoble Alpes, SIMAP, CNRS, 38000 Grenoble, France

Keywords:
Chromium coatings
MOCVD
Cr metastable phase
Structural transformation
Tracer
Hard coatings

A B S T R A C T

Cr deposits are widely used as protective coatings but multifunctional performances are required in harsh environments motivating research on new processes. MOCVD of Cr metal coatings was carried out by direct liquid injection (DLI) of a unique solution containing bis(ethylbenzene)chromium as metal source and thiophenol as inhibitor of carbide formation. A low amount (<6%) of the metastable δ-Cr phase was found embedded in the stable α-Cr phase. The formation of this metastable phase originates from both the low deposition temperature (<723 K) and the use of thiophenol. It was not reported under other CVD conditions. Dense coatings were deposited by implementing a multilayer growth mode. Such coatings exhibit a high nanohardness of about 17 GPa. The δ-Cr metastable phase undergoes an irreversible structural transformation to bcc-Cr above 723 K. The mechanical properties of coatings are not affected by the structural transformation because of the similarity of their crystallographic structures (both cubic), their density very close (a volume contraction of only 0.4% during the transformation) and its low content. This metastable phase is a signature of the DLI-MOCVD process and it can be used as a tracer for Cr coatings operating in high temperature environment without loss of the basic properties.

1. Introduction

In order to grow protective metallic chromium coatings, wet routes generally use a lot of toxic chemicals including chromic acid solutions based on hexavalent chromium [1–3] which is now forbidden by REACH regulation. Several alternatives are investigated using trivalent chromium [4,5] but they should also result in a regulation ban.

At the opposite, it is possible to deposit chromium coatings by PVD processes as cathodic magnetron sputtering [6,7], cathodic arc evaporation [8], hollow cathode discharge [9] and high power impulse magnetron sputtering (HIPIMS) [10] without using dangerous chemicals. The main drawbacks of these physical methods are their complexity for the deposition on large pieces, the relatively low growth rates and finally the fact that they are line-of-sight deposition techniques, which excludes conformal and uniform coatings on three dimensional objects.

CVD processes are well suited for conformal growth on complex shapes. Their drawback comes from the high working temperatures using traditional halides precursors. For instance, Cr metal coatings are deposited by pack cementation above 1300 K [11–13]. However, by using metalorganic compounds (MOCVD), the deposition temperature is significantly decreased, for instance below 773 K for Cr-based coatings depending on the precursor [14,15], and even at 523 K using reactive *tetra*-alkylchromium complexes [16]. As a result, thin film deposition on a wide variety of substrate materials is possible without structural and dimensional changes. In spite of a C-rich vapor phase originating from the organic ligands of the precursor, metallic Cr thin films can be deposited by MOCVD using inhibitors of carbon incorporation and carbide formation as chlorinated [14,17–20] and sulfur-containing derivatives [21].

An even more surprising challenge was to find that when the emerging technology of direct liquid injection (DLI) is implemented for supplying a cold-wall reactor operating under atmospheric pressure with high vapor flow rates, the carbon incorporation inhibitors were still effective while large amounts of hydrocarbon solvent were injected with the precursor [22–24]. Indeed DLI-MOCVD is an alternative process where the precursor is diluted or dissolved in a liquid organic solvent. This solution is then injected

* Corresponding author at: CIRIMAT, ENSIACET, 4, allée Emile Monso, BP 44362, 31030, Toulouse cedex 4, France.
E-mail address: francis.maury@ensiacet.fr (F. Maury).

as a pulsed spray in a flash vaporization chamber and the reactive gas phase is transported by a carrier gas to the CVD reactor. This technique generates highly stable and controlled vapor flow rates of the precursor leading to relatively high growth rate at low temperature (<773 K). An appropriate choice of precursor provides high yields [15]. Thus, DLI-MOCVD process for Cr deposition has been successful using C_6Cl_6 [22–24] and C_6H_5SH [24] as inhibitors and bis(arene)chromium as metal source.

The microstructural characteristics and therefore the properties of chromium coatings depend on both the processes used and the deposition conditions. There are two different crystalline phases of chromium in standard conditions. The first one corresponds to the stable bcc cubic structure with *Im-3m* (229) space group and 2.88 Å cell parameter (PDF 00-006-0694), noted bcc-Cr (or α-Cr). The second one is a primitive cubic metastable phase with *Pm-3*n (223) space group and 4.59 Å cell parameter (PDF 00-019-0323) [25,26], noted δ-Cr.

Except high-temperature CVD processes that produce thermochemical diffusion coatings, most of the above cited processes, including DLI-MOCVD, lead to the formation of α-Cr thin films, although the growth conditions are far from thermodynamic equilibrium. The processes leading to the growth of the metastable phase are rare. Evaporation and condensation of chromium in argon at low pressures [25–27] led to the formation of crystalline metastable δ-Cr. The same authors reported the structural transformation of the metastable phase to the stable one above 723 K.

The aim of this paper is to study Cr coatings deposited at temperatures below 723 K in a hot-wall DLI-MOCVD reactor. We show they have the particularity of containing small amounts of metastable δ-Cr phase embedded in α-Cr polycrystalline matrix. Furthermore, these Cr coatings are supersaturated with carbon which gives them unusual metallurgical properties. The resulting high nanohardness makes them good candidates as hard protective coatings. This work also demonstrates that for applications in harsh environments, if the operating temperature exceeds 723 K, the metastable phase irreversibly transforms into the stable bcc phase, acting as a tracer without loss of the basic properties of the coating.

2. Experimental

2.1. Deposition process

Depositions were carried out by DLI-MOCVD in a horizontal, hot-wall, pyrex tubular reactor (300 mm long and 24 mm internal diameter) with an isothermal zone around 150 mm. Si(100) and stainless steel (304L) plates were used as substrates and placed on a planar horizontal substrate-holder in the isothermal zone. The total pressure was kept constant at 6.7 kPa and the growth temperature was fixed at either 673 (400 °C) or 723 K (450 °C).

Commercial BEBC, bis(ethylbenzene)chromium (from Strem Chemicals, CAS 12212-68-9, in fact a mixture of $[(C_2H_5)_xC_6H_{6-x}]_2Cr$ where x = 0–4) was used as chromium precursor. It is a viscous liquid that was mixed with anhydrous toluene (99.8% from Sigma-Aldrich, CAS 108-88-3) at 3×10^{-1} mol L^{-1} (4 g of BEBC in 50 mL of toluene). A sulfur-containing inhibitor of carbon incorporation, thiophenol, C_6H_5SH (from Sigma-Aldrich, purity > 99%), was introduced into this solution with a mole ratio n_{thiol}/n_{BEBC} = 2% to grow preferentially Cr metal coatings instead of chromium carbide coatings.

The liquid solution containing both the precursor and the inhibitor was injected in a flash vaporization chamber (473 K) at 0.9 mL min^{-1} by appropriately tuning injection parameters (frequency and opening time). Nitrogen was used as carrier gas with a 500 sccm flow rate and was heated at 453 K before entering the flash vaporization chamber to prevent condensation.

Table 1
Growth conditions of Cr metal coatings by DLI-MOCVD in a horizontal hot-wall reactor using an injection of a single solution of BEBC and thiophenol in toluene, as chromium source and inhibitor of carbide formation, respectively.

Coating type	Monolayer	Multilayers (9 layers)
Deposition temperature (K)	673; 723	673; 723
Total pressure (kPa)	6.7	6.7
Carrier gas N_2 (sccm)	500	500
Solvent	Toluene	Toluene
BEBC concentration (mol/L)	3.5×10^{-1}	3.5×10^{-1}
Thiophenol concentration (mol/L)	7.0×10^{-3}; 3.5×10^{-2}	7.0×10^{-3}
Injection feed rate (mL/min)	0.9	0.4
Injection frequency (Hz)	10	3
Opening time of injector (ms)	0.5	0.5
Growth duration (min)	60	140

In a first mode, coatings were deposited as monolithic layers, namely monolayers, by keeping constant all the conditions during the deposition run. However the first analyses revealed a columnar morphology with a high porosity between the columns which is not suitable for protective coatings. In order to increase the compactness, in a second deposition mode, the coatings were structured in multilayers by stopping the precursor injection for 5 min every 15 min without significant temperature change or venting. The temporary shutdown of the growth created clean interfaces. At the beginning of each injection period a new nucleation step and crystal growth occurred and was stopped before the formation of the columns, *i.e.* after 15 min, which limits the thickness of individual layers and hinders the development of columns. Thus, dense multilayer coatings with 9 layers were produced. Characterizations will be shown for both types of coatings. Table 1 details the experimental deposition conditions.

2.2. Coating characterization

The morphology of the Cr coatings were characterized by scanning electron microscopy (SEM; Leo-435VP) and their microstructure was studied by Electron Back Scattered Diffraction (NordlysNano EBSD Detector with the AZtecHKL software installed on a SEM-FEG JEOL JSM-7100TTLS LV) and TEM (JEOL JEM 2100 equipped with a 200 kV FEG). Their crystalline structure and thermal stability were analyzed by XRD and in-situ XRD vs temperature under Ar atmosphere, respectively (Bruker D8-2 diffractometer equipped with a graphite monochromator; Bragg-Brentano configuration; Cu Kα radiation).

The film composition was analyzed by electron probe microanalysis (EPMA; Cameca SXFive, 15 kV and 20 nA) and the chemical environment of each element of the coating was investigated using an XPS spectrometer (Thermo Scientific K-Alpha), equipped with a monochromatic Al X-ray source and a low energy Ar^+ gun (1 keV) for surface cleaning and depth profile analysis. Rutherford Backscattering Spectrometry (RBS; 1.5 MeV H^+ beam; detection at 160°) was used to estimate the density of coatings.

3. Results and discussion

3.1. Deposition of the bcc-Cr stable phase

Many CVD reactor configurations and sizes, as well as deposition conditions have been previously tested to deposit metallic Cr [14,17–24]. These studies on MOCVD and DLI-MOCVD processes are summarized in Table 2. In the case of DLI-MOCVD process, the presence of a large amount of hydrocarbon solvent vapor is worth noting. Experimental sets involving (i) addition of a reactive gas (H_2) to the inert carrier gas (N_2), (ii) hot-wall and cold-wall reactor configurations, (iii) bis(benzene)chromium (BBC)

Table 2
Experimental conditions used for Cr deposition by MOCVD and DLI-MOCVD. Bis(benzene)chromium (BBC) and bis(ethylbenzene)chromium (BEBC) were used as precursors and either C_6Cl_6 or C_6H_5SH were used as inhibitors of carbide formation.

Process	Reactor[a]	Carbon inhibitor	BBC				BEBC			
			Atm[b]	P (kPa)	T (K)	Ref.	Atm[b]	P (kPa)	T (K)	Ref.
MOCVD[c]	hw	C_2Cl_6; C_6Cl_6	–	–	–	–	nr	nr	573–748	[17]
MOCVD[c]	hw	$(C_6H_5CH_2)_2S$; $(C_6H_5)_2S$	–	–	–	–	vacuum	1.3×10^{-3}	573–723	[21]
MOCVD	cw	C_6Cl_6	H_2	0.8	673	[14]	–	–	–	–
MOCVD	hw	C_6Cl_6	H_2	0.4–2.0	573–673	[14,18,19]	H_2	0.8	623	[18]
DLI-MOCVD	cw	C_6Cl_6	Tol; Cyclo	6.7; 101	753–793	[22,23]	–	–	–	–
DLI-MOCVD	hw	C_6Cl_6	Tol	6.7	748	[24]	–	–	–	–
DLI-MOCVD	hw	C_6H_5SH	Tol	6.7	748	[24]	–	–	–	–
DLI-MOCVD	hw	C_6H_5SH	Tol	6.7	723	This work	Tol	6.7	673; 723	This work

[a] cw means cold-wall vertical reactor and hw means hot-wall horizontal tubular reactor.
[b] Atm means atmosphere; Tol and Cyclo mean toluene and cyclohexane used as solvents to inject the precursor solution.
[c] The precursor used, namely Barkhos was a mixture of bis(arene)chromium slightly different from the BEBC (nr means not reported).

or bis(ethylbenzene)chromium (BEBC) as bis(arene)chromium(0) precursor, (iv) different carbide inhibitors, (v) total pressure range from atmospheric to low pressure (0.4 kPa), and (vi) growth temperature range from 573 to 793 K were studied. The main reason to explore the effects of all these conditions comes from the key role played by surface chemistry for the competitive deposition of metallic Cr and carbides. Obviously this surface chemistry can be influenced by the gas phase chemistry which can be dependent on experimental conditions and reactor configurations.

So far, MOCVD and DLI-MOCVD processes only led to the growth of single-phase polycrystalline bcc-Cr coatings. This is the stable body-centered cubic structure of the metal (space group *Im-3m*). This common phase was obtained by adding a chlorinated [14,17,22,24] or a sulfur-containing [21,24] inhibitor to the bis(arene)chromium precursor. The present work complements these previous studies and is distinguished on several points: (i) the DLI-MOCVD process was used, (ii) with BEBC and C_6H_5SH in a unique solution containing both the precursor and the inhibitor, (iii) H_2 was not added in the reactive gas phase, (iv) a larger CVD reactor was used, and (v) operating temperatures were lower than 723 K, as specified in Table 2.

A monolayer coating deposited according to mode 1 at 723 K by DLI-MOCVD on silicon substrate exhibits typically a columnar and porous chromium structure. It is generally composed of the stable bcc crystalline phase. No evidence of carbide formation was found by XRD. The SEM micrograph of Fig. 1a shows a 5.7 μm thick coating consisting of disjoint columns perpendicular to the surface of about 1 μm wide grown from a denser 1 μm thick sub-layer where the columns are not yet formed. The corresponding XRD pattern in the 2θ range 35–80° exhibits the two main peaks of the stable bcc-Cr at 44.4° (110) and 64.6° (200). The Kα2 contribution can also be seen as a shoulder of the (200)Cr peak, as well as the Kβ contribution for the most intense (110)Cr peak (Fig. 1b). This stable bcc-Cr phase exhibits a preferential orientation of the growth along the [110] direction with a texture coefficient of 1.8 which is consistent with a columnar morphology.

As expected, the coatings deposited according to the mode 2 have a multilayer structure with a greater compactness and a smoother surface morphology compared with monolayer coatings. Fig. 2 shows a cross-section view of a cleaved sample on Si substrate grown at 673 K. It consists of 9 layers with clear interfaces and the total thickness is 3.4 μm. The average grain size is lower and less dispersed than for mode 1; typically of the order of magnitude of the thickness of the individual layers (≤380 nm).

The interfaces are clear between each layer because the stopping of the injection lasted long enough (5 min) to make the transient effects negligible and to suppress any nutrient species for the growth of the coating. Indeed, the evacuation of the gaseous reactants is rapid under a total pressure of 6.7 kPa and maintaining the carrier gas flow rate (500 sccm) during the stopping of the precursor injection ensures an efficient purge of the reactor.

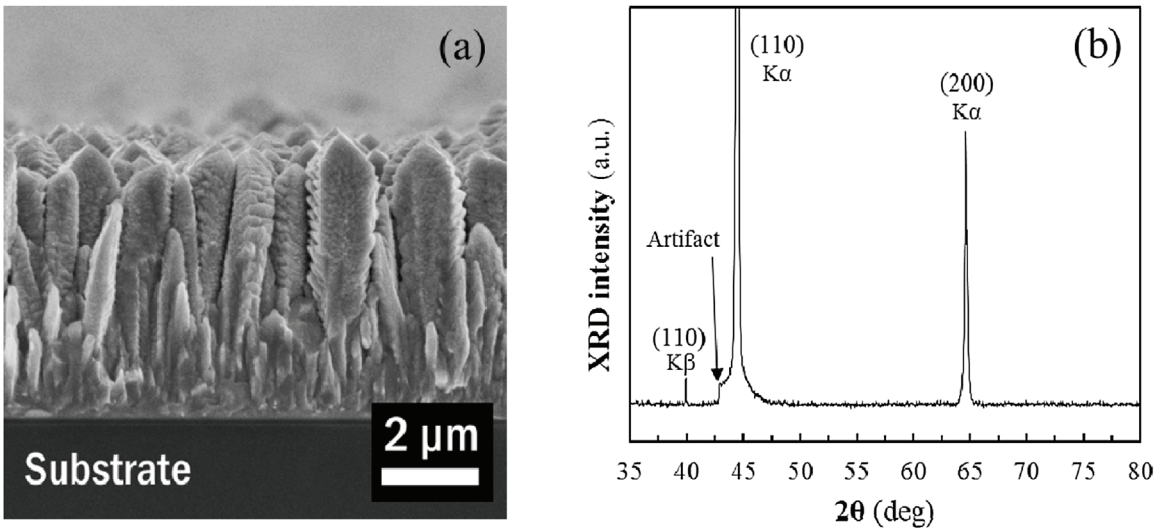

Fig. 1. (a) SEM micrograph of a cross-section and (b) corresponding XRD pattern of a monolayer Cr coating deposited on Si substrate by DLI-MOCVD according to mode 1 (723 K; 6.7 kPa; inhibitor C_6H_5SH). The coating is single-phased and exhibits a textured bcc-Cr structure.

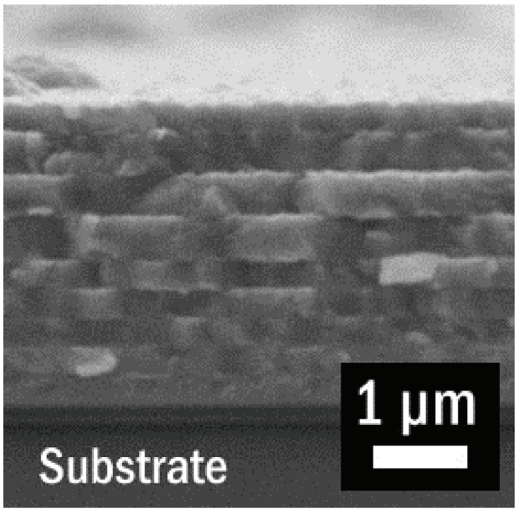

Fig. 2. SEM micrograph of the cross-section of a two-phase multilayer coating grown at 673 K and 6.7 kPa on Si substrate (according to mode 2) showing the 9 layers composing it and its high compactness.

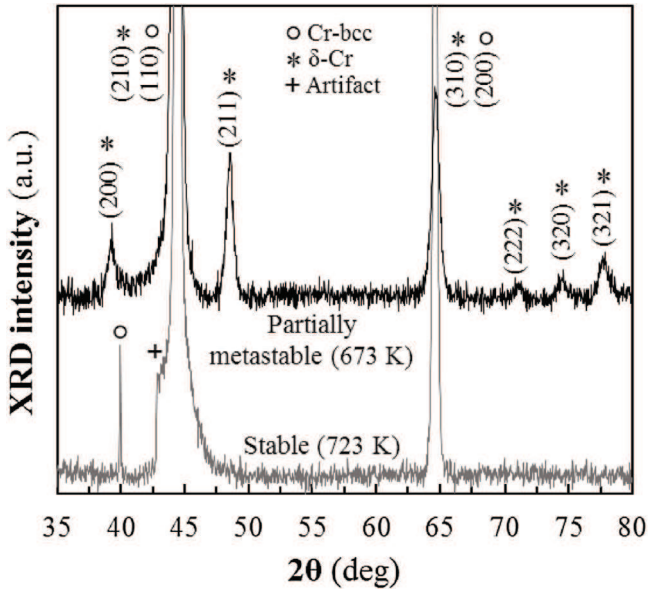

Fig. 3. XRD patterns of a two-phase coating comprising the metastable δ-Cr phase and the stable bcc-Cr phase (top and black pattern; multilayer coating) and of a stable bcc-Cr monolayer coating (bottom and grey pattern) deposited by DLI-MOCVD on Si substrate, respectively at 673 K and 723 K (other conditions: 6.7 kPa; C_6H_5SH).

About the transient effects induced by these multilayer deposition conditions, transient changes can be expected for temperature and pressure. However the total pressure is independently and automatically regulated at a fixed value and it does not affect the microstructure of coatings when it is varied in a narrow range. As a result, the transient changes of pressure induced by this stepwise delivery of precursor are insignificant. Regarding the substrate temperature, the temperature profile calculated in this 3-dimensionnal reactor showed a cold finger at the entrance of the reactor over a few centimeters originating from the injection of colder vapor phase (473 K). The stopping of the injection of the precursor solution in the toluene decreases the total flow rate of the gas phase by about 30% (about 750 sccm compared to 500 sccm with and without precursor injection respectively) and consequently substantially reduces the length of this temperature gradient zone at the entrance. This transient effect on the temperature is not harmful since it expends the isothermal zone of the reactor.

By combining the atomic density measured by RBS with the thickness of the coating (2 μm) measured by SEM and its atomic composition measured by EPMA, a density of $7.7 \pm 0.6\ g/cm^3$ was found. Usually the density of coatings is lower than that of bulk materials. Despite a significant experimental error, the density measured is of the same order of magnitude as that of bulk bcc-Cr ($7.19\ g/cm^3$). This confirms the high density of DLI-MOCVD Cr multilayer coatings grown according to mode 2.

Chemical analyses of previous MOCVD and DLI-MOCVD coatings typically revealed a low carbon content (from 3 to 8 at.%) [14,22,24] and a slight contamination by oxygen because of a residual oxygen in the reactor or impurities in the precursor and inhibitor. Depending on the growth conditions, coatings also contain a small amount of chlorine (<1 at%) or sulfur (<3 at%) originating from the inhibitors of carbide formation.

In this work, the two types of coating deposited according to modes 1 (monolayer) and 2 (multilayer) using thiophenol as inhibitor of carbon incorporation have similar compositions which are in good agreement with previous studies [14,22,24]. For instance, EPMA analysis of multilayer coatings deposited at 673 and 723 K under low pressure (6.7 kPa) and using a mole ratio thiophenol/BEBC equals to 2% in the injected solution have the composition $Cr_{0.92}C_{0.04}O_{0.03}S_{0.01}$.

3.2. Evidence of the metastable phase δ-Cr

For all previous MOCVD films deposited at 623 and 673 K with C_6Cl_6 as inhibitor, the stable bcc-Cr phase was the only one identified by XRD [14,18,19]. The same result was found by DLI-MOCVD using C_6Cl_6 in the temperature range 748–793 K [22–24]. The coatings grown at 748 K using thiophenol as inhibitor also exhibit a single-phase bcc structure [24]. In the present work, thin film growth by DLI-MOCVD using thiophenol at 673 and 723 K allowed to observe the formation of two crystalline phases: the stable bcc-Cr one and the metastable δ-Cr phase which has a cubic structure (space group *Pm-3n*) with a larger lattice parameter of 4.59 Å. The XRD pattern of a partially metastable coating grown at 673 K according to mode 2 (multilayers) is shown in Fig. 3 and compared with a pure stable bcc-Cr monolayer coating grown at 723 K (mode 1).

For multilayer coatings deposited at 673 K, both stable and metastable phases are identified, whatever the substrate used (Si or stainless steel). The stable bcc-Cr phase shows a polycrystalline structure consisting of well crystallized grains whose average size is large enough (>300 nm) not to induce a measurable widening of the XRD peaks. On the contrary, the XRD peaks of the metastable δ-Cr phase have large FWHM which reflects the nanometric average size of the crystallites, estimated at 17 and 28 nm using the Scherrer equation from the peaks (211) and (200), respectively.

From the relative intensity of experimental XRD peaks (I_{hkl}) of Fig. 3 compared to those of PDF files of randomly oriented coatings (I^0_{hkl}), a texture coefficient (T_{hkl}) for both phases was calculated according to $T_{hkl} = (I_{hkl}/I^0_{hkl})/[n \cdot S(I_{hkl}/I^0_{hkl})]$, where n is the number of diffraction peaks considered in a given angular range. Contrarily to coatings grown in the monolayer mode, multilayer coatings grown at 673 K do not exhibit preferential orientation for the dominant bcc-Cr phase; $T_{110} = 0.9$ compared to 1.8 for the monolayer coating. This is directly the result of the multilayer structure which hinders the columnar growth, decreases the average grain size and subsequently leads to a higher density of coatings. For this two-phase coating, the metastable phase δ-Cr exhibits a noticeable preferential orientation in the [211] direction with an estimated

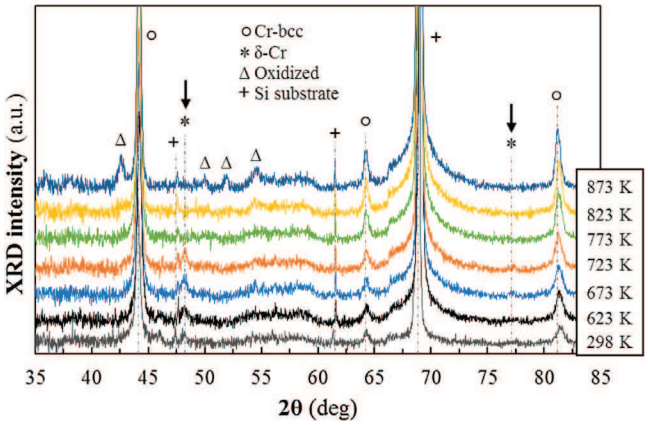

Fig. 4. In situ XRD of a partially metastable chromium monolayer coating at different temperatures under Ar atmosphere (deposition at 673 K and 6.7 kPa on Si substrate). Arrows show disappearance of the metastable δ-Cr phase. The sample was heated with a temperature ramp of 1 K min^{-1} and it was maintained 35 min at each temperature to record the pattern.

texture coefficient of 1.8 despite the low intensity of the diffraction peaks.

The XRD peaks of the metastable phase are always less intense than those of the stable phase, indicating small amounts. From the ratio of the relative XRD intensity of the most intense peaks of δ-Cr (211) and bcc-Cr (110), and so neglecting the low texture of the metastable phase, a coarse proportion of δ-Cr was estimated at about 6%. This method suffers from two approximations; (i) the low texture of δ-Cr overestimates the intensity that should be considered for δ-Cr(211) and (ii) the crude intensity of bcc-Cr(110) is also overestimated because of overlap with the δ-Cr(210) peak. Interestingly, both approximations compensate what makes sense to the method.

In situ XRD analyses allowed us the verification of the thermal stability, in argon atmosphere, of the metastable phase embedded in the stable bcc matrix. The arrows on XRD patterns of Fig. 4 show the complete transformation of the metastable δ-Cr phase into the stable bcc-Cr one beyond 723 K, in good agreement with literature data [25–27]. Traces of chromium oxide appear above 823 K, mainly due to the residual oxygen partial pressure in the XRD analysis chamber. On returning to room temperature, the XRD pattern is the same as at 873 K confirming that the δ-Cr → α −Cr transformation is irreversible. From this series of XRD patterns recorded in situ on a diffractometer different from that of Fig. 3, the mean crystallite size estimated with the δ-Cr(211) peak is 21, 32 and 30 nm at the temperatures 623, 673 and 723 K respectively. These values are consistent with that measured at room temperature with data of Fig. 3. No significant variation of the average size of δ-Cr crystallites was found for this heat treatment. Above 723 K, the metastable phase disappears.

No evidence for the metastable δ-Cr phase was found by TEM analysis, probably because of the very low amount of this phase compared to the stable one. Another hypothesis is that it could undergo a phase transformation under the TEM 200 kV electronic beam. Electron-beam induced phase transformation is a well-known phenomenon as reported in several papers relative to metallic alloys [28], minerals [29] or oxides [30].

Fig. 5 illustrates a TEM analysis of a two-phase monolayer coating characterized by a columnar morphology. A Precision Ion Polishing System (PIPS) was used to prepare the sample, resulting in a thin slice of the coating approximately parallel to the surface of the film. Therefore Fig. 5a shows a cross-section of one column (and a part of another one) perpendicular to its longitudinal axis. The insert in Fig. 5b presents the corresponding electron diffraction pattern attributed to the stable bcc phase with [011] zone axis. An experimental lattice parameter of 2.92 Å was deduced from electron diffraction patterns of several crystallites in good agreement, within 2%, with the literature value of bcc-Cr (2.88 Å). A high-resolution picture in the same area shown in Fig. 5c reveals a very homogeneous packing. Its Fourier transform in the insert (d) is in agreement with the experimental pattern in (b). Moreover, columns observed by TEM appear polycrystalline in agreement with the fact that the texture is not very important even if it exists for monolayer coatings (Fig. 1b). The cross-section confirms these columns have an average diameter of about 1 μm, as found in SEM observations (Fig. 1a).

A two-phase multilayer coating comprising the metastable component was analyzed by SEM, coupled to an EBSD detector. It is in fact a cross-section of this multilayer coating prepared with a cross-section polisher (JEOL IB-19510CP) which was studied. An EBSD band contrast example is presented on Fig. 6a. It is similar to classical secondary electrons SEM images, as shown in Fig. 2, except that the contrast makes it easier to see the grains. EBSD phase mapping is shown in Fig. 6b. The stable bcc-Cr and metastable δ-Cr phases are identified with two distinct colors, respectively blue and red.

EBSD statistical analysis was performed on approximately 1000 grains. Identification of both metastable and stable Cr phases was possible. The metastable δ-Cr phase proportion is around 3%. This compares quite well with the 6% determined by XRD assuming that both phases were not textured. The metastable phase is essentially found at interfaces of the multilayer and at grain boundaries of the dominant bcc phase where there is the highest density of structural defects and in low EBSD signal areas. It was complicated to discern the two phases because they have the same composition and both exhibit cubic structures (bcc for the stable phase and primitive cubic for the metastable one). In this two-phase multilayer coating, the average grain size of bcc-Cr is approximately 300 nm while it is only a few nanometers for δ-Cr. In a previous work, It was reported that the particles of this metastable δ-Cr phase did not exhibit a definite crystal shape and their average size was lower than 20 nm [26].

No specific grain orientation was observed by EBSD analysis for the stable bcc phase, as it can be seen on the inverse pole figure in Fig. 6c. This confirms that no preferential orientation of the growth occurs using this multilayer CVD mode. This result is in very good agreement with XRD analysis which showed the absence of texture for the stable phase with a texture coefficient of 0.9 for the [110] direction (Fig. 3).

XPS analyses were performed to study the environment of atoms and analyze the nature of impurities in these coatings. A survey scan after the surface cleaning by Ar^+ sputtering, reported as supplementary information, reveals the presence of only Cr, O, C and S (Fig. S1). It is not possible to distinguish α-Cr from δ-Cr. Fig. 7 presents XPS region spectra of Cr 2p, O 1s, C 1s and S 2p levels from a two-phase multilayer Cr coating deposited on a Si substrate. Three different sputtering times are displayed for each electronic level: 0 s (as-deposited), 120 s and 2012 s. As-deposited sample exhibits a surface contamination containing chromium oxides (Cr $2p_{3/2}$ at 576.6 eV and O 1s at 530.8 eV), adventitious carbon (C 1s at 284.8 and 288.3 eV) and sulfate anions (S $2p_{3/2}$ at 168.7 eV).

For the longest cleaning time by sputtering, this contaminated surface is sufficiently cleaned and data are more representative of the coating composition. The main contribution of Cr $2p_{3/2}$ is shifted to 574.0 eV which is characteristic of metal Cr, even if an overlap exists with a small contribution due to Cr—C bonds (Fig. 7a). Traces of oxygen lead to a response of Cr—O bonds as a shoulder at 576.6 eV for Cr $2p_{3/2}$ and a contribution to O 1s at 530.8 eV (Fig. 7b). This oxygen was attributed to a slight oxidation of the coatings in agreement with EPMA data (3 at%). Fig. 7c shows carbon incorporated in two

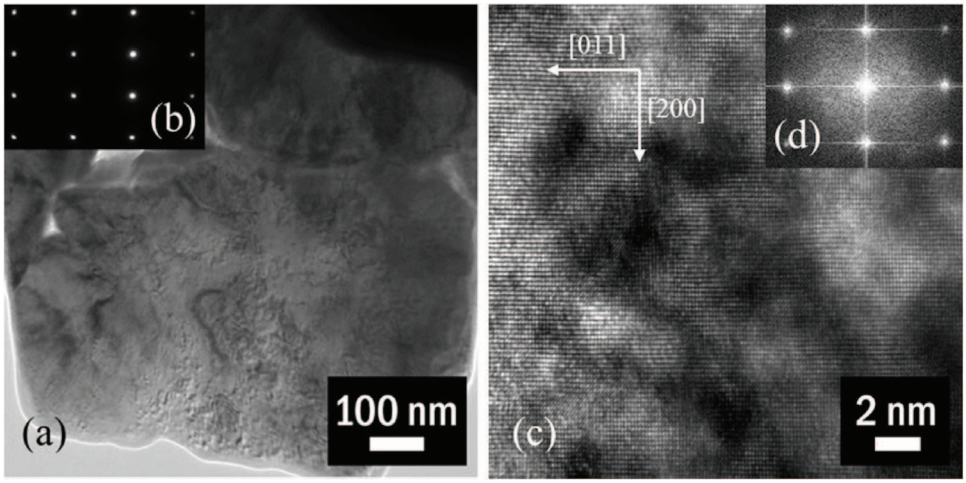

Fig. 5. (a) TEM observation of a two-phase monolayer Cr coating; (b) corresponding selected area electron diffraction pattern ([011] zone axis); (c) High resolution micrograph; (d) corresponding Fourier transform of the high-resolution view.

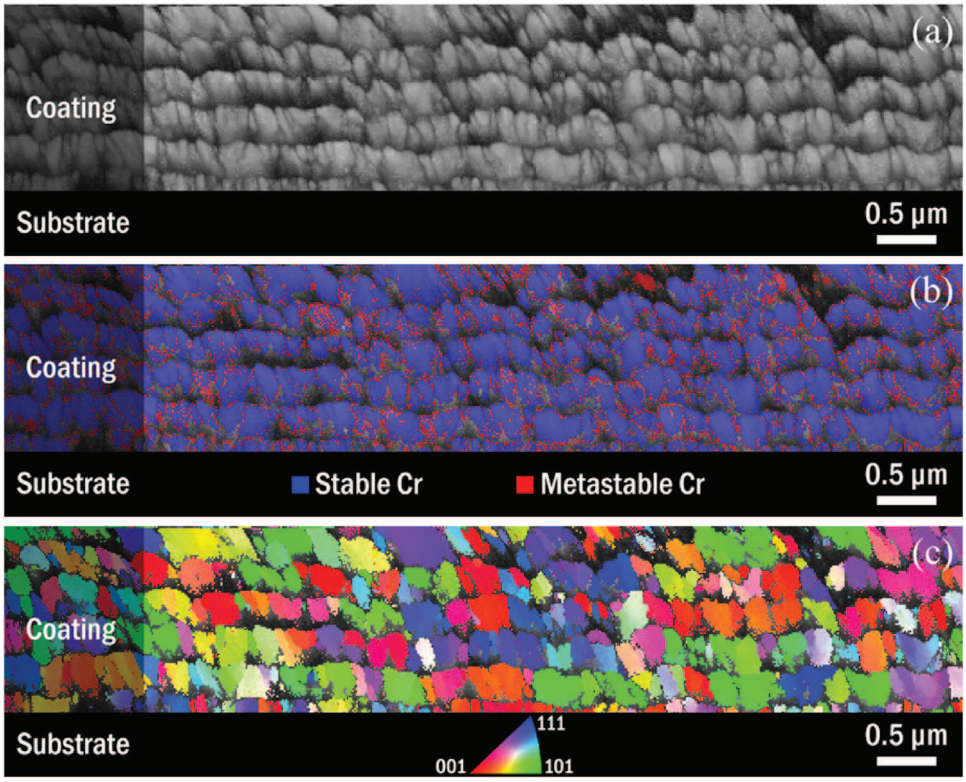

Fig. 6. EBSD analysis of a cross-section of a two-phase multilayer coating grown at 673 K and 6.7 kPa on Si substrate: (a) band contrast; (b) phase mapping; (c) inverse pole figure (z axis).

forms: as free carbon (C 1s at 284.6 eV, dominant contribution) and as carbide (C 1s at 282.8 eV). By combining the relative intensity of free C and carbide components with the total C content determined by EPMA (4 at%), the amount of C in the carbide form is estimated at about 0.8 at%. This is significantly higher than C solubility in Cr which was reported to be <0.1 at% at about 750 K [31].

After surface cleaning, the S 2p level, although not very intense, gives evidence for a unique environment in the form of S—Cr bonds with S $2p_{3/2}$ shifted at 161.6 eV, with a shoulder at 162.8 eV for S $2p_{1/2}$ (Fig. 7d). This is characteristic of metal sulfide or of S solubilized in the metal structure. In this sample, total S content analyzed by EPMA was only 0.5 at% which is higher than the solubility of sulfur in chromium at 673 K [32]. Consequently a sulfide contamination likely exists but the amount is too low to be analyzed by XRD or TEM.

3.3. Origin of the metastable phase δ-Cr

The metastable phase δ-Cr was clearly identify in small amount by XRD and EBSD in DLI-MOCVD Cr metal coatings deposited both in mode 1 (monolayer) and mode 2 (multilayer). It is better visible in multilayer coatings than in monolayer because the columnar growth and textured structure in the latter make it difficult to observe, since the relative intensity of δ-Cr XRD peaks is crushed by that of the preferential orientation of α-Cr. Several factors seem to influence the formation of this metastable phase.

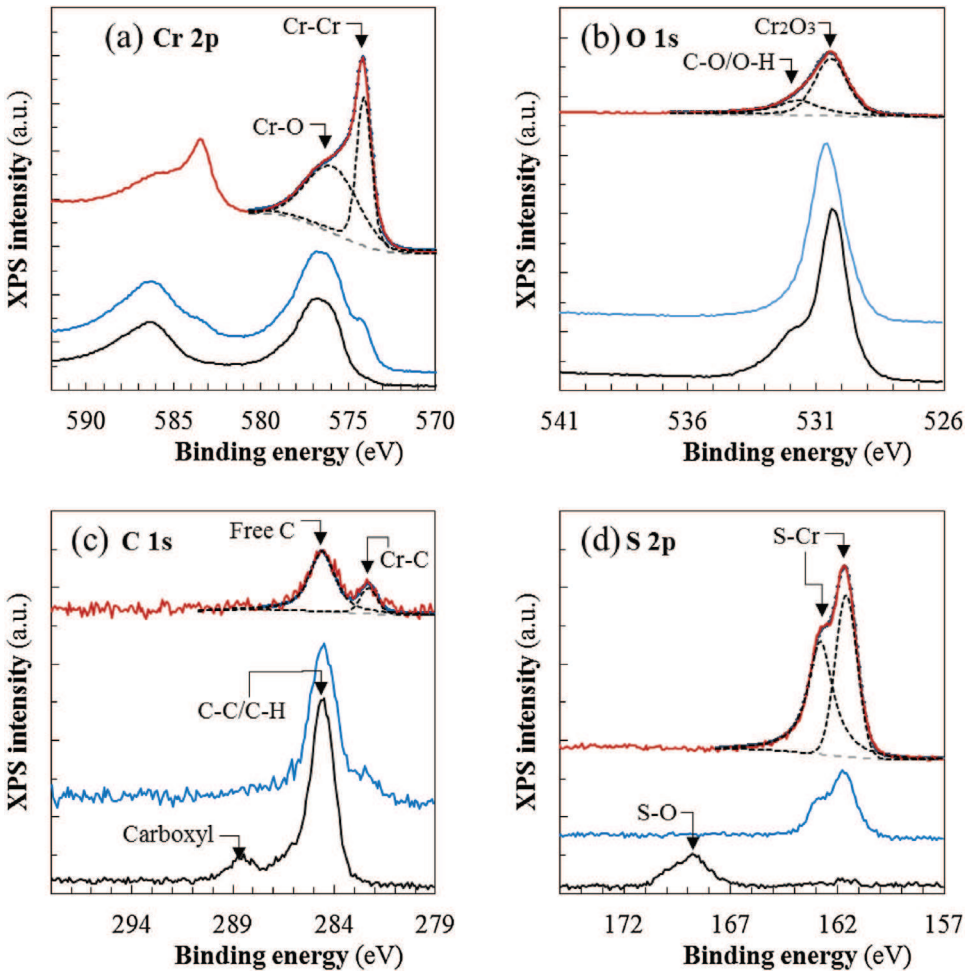

Fig. 7. XPS analyses of a two-phase multilayer Cr coating comprising the metastable δ-Cr and the stable α-Cr phases deposited at 673 K. Spectral regions of (a) Cr 2p, (b) O 1s, (c) C 1s and (d) S 2p are reported for different Ar^+ sputtering times (1 keV): 0 s (as-deposited; black spectrum, bottom), 120 s (blue, middle) and 2120 s (red, top). An offset along the Y axis has been applied for clarity and a deconvolution of the most representative spectrum of the coating is plotted. (For interpretation of the references to colour in this figure legend, the reader is referred to the web version of this article.)

It was never reported in Cr coatings grown by MOCVD and DLI-MOCVD using chlorinated inhibitors [14,17–19,22–24] even for deposition temperature as low as 573 K. When using sulfur-containing inhibitors it was not mentioned by MOCVD [21] nor by DLI-MOCVD [24] (Table 2). It has been observed in this work by DLI-MOCVD using C_6H_5SH as inhibitor of carbon incorporation only for deposition temperature ≤723 K. This is in good agreement with the fact that beyond this critical temperature a structural phase transformation into bcc-Cr occurs, as reported by [25–27] and confirmed by in situ XRD analysis in this study (Fig. 4).

When the deposition is carried out at 723 K, the observation of this phase depends on the position of the samples in a quasi-isothermal reactor, which means it depends on the local deposition conditions, *i.e.* mainly on the substrate temperature. Numerical modeling (not reported here) showed for our DLI-MOCVD reactor that when the temperature of the furnace is set to 723 K, the substrate temperature was approximately 50 K lower, *i.e.* around 673 K. This temperature decrease comes from of the presence of a cold finger at the entrance of the reactor over several centimeters in the axial direction [33]. This is due to the lower temperature of the reactive gas phase (approximately 473 K) coming from the flash vaporization chamber which enters the reactor. Consequently, the formation of the metastable phase is then possible because the substrate temperature is lower than the critical value beyond which the structural transformation occurs. For the same furnace temperature (723 K), but using another geometry and size of the CVD reactor different transport conditions have to be used leading to different temperature fields. Consequently, the temperature difference between the substrate and the furnace set-point will be different than in this work and the metastable phase may not be observed if the reactor is more isothermal. This is consistent with a sharp structural phase transformation at this critical temperature of 723 K. So, for the deposition of metallic Cr coatings containing δ-Cr as a minor phase, DLI-MOCVD is a suitable process. The substrate temperature must be lower than 723 K and C_6H_5SH is the best inhibitor.

Structural phase transformation in metals induced by impurities is a common phenomenon [34]. Moreover, magnetic ordering of chromium is affected by impurities (doping) which induces changes in phase transition [35]. Thiophenol likely promotes the formation of the metastable phase. Sulfur impurities are incorporated in the coating (< 1 at.%) and they could induce the structural phase transformation within Cr coatings. Thiophenol action was found efficient starting from a mole ratio thiophenol/BEBC of 2% (the tested values were in the range 1–10%). For a mole ratio of only 1%, no inhibitory action was observed since the formation of chromium carbides occurred instead of metallic chromium.

The relatively large FWHM of XRD peaks of δ-Cr phase together with the EBSD analysis gives evidence that this metastable phase is present in the form of nanocrystallites. The nanometric size of

δ-Cr particles may be another cause of its stability. Indeed such a nanometric effect is known for instance to stabilize the metastable anatase form of titania relative to rutile although this last one is thermodynamically the most stable phase. This is because the surface energy of anatase is significantly lower leading to stable anatase nanoparticles below a critical size of about 15 nm [36]. Our observation of δ-Cr only in the form of nanoparticles is consistent with [26] where authors also reported δ-Cr as nanoparticles, which could be explained by a lower surface energy than that of bcc-Cr.

As mentioned above the δ-Cr phase is more easily seen in multilayer coatings than in the monolayer coatings. Furthermore, EBSD analyses have shown that it is located both at the interfaces and grain boundaries (Fig. 6). From fundamentals of nucleation and crystal growth it can be assumed that the metastable phase deposition is controlled by a heterogeneous nucleation step rather than a steady state growth regime because the surface seems to play an important role and its crystallite size stays limited at the nanometric scale. This hypothesis suggests that its proportion would increase with the number of grain boundaries and interfaces as obtained in the multilayer coatings. So by increasing the nanostructuration which means by increasing the number of individual layers in the coating, the number of both grain boundaries (due to lower average crystallite size) and interfaces will increase, which could favor the growth of δ-Cr. This idea has not yet been verified. From the XRD pattern of Fig. 3, the proximity of the most intense peaks of each phase suggests that an epitaxial relationship may exist which would favor the nucleation of δ-Cr(211) plane on α-Cr(110) and would explain the preferential orientation of δ-Cr in the [211] direction.

3.4. Unusual properties

These DLI-MOCVD Cr coatings are promising candidates as protective metallurgical coatings. They are deposited at low temperature (T < 723 K) with a relatively high growth rate (~5 μm/h). The multilayer coatings exhibit a density as high as that of bulk metallic Cr (7.19 g/cm^3). For applications in harsh environments, if the operating temperature incidentally exceeds 723 K, the metastable phase will be irreversibly transformed into the stable bcc phase (Fig. 4). According to their crystallographic structures, the metastable δ-Cr phase is slightly less dense than α-Cr (7.16 g/cm^3). This means that at the time of the phase transformation the overall volume contraction will be only 0.4%. Furthermore the proportion of δ-Cr does not exceed 6% in multilayer coatings as deduced from XRD and EBSD analyses. This indicates that it can act as a tracer likely without loss of the basic properties of the coatings. This is particularly useful in non-destructive testing of manufactured structural components protected with such a coating.

Indeed carbon-steels and alloys undergo specific heat treatments to optimize their mechanical properties (ductility, hardness...) and their operating temperature must not exceed the temperature of the last treatment undergone as hardening or tempering annealing. Beyond the critical temperature a steel structure cannot carry the service load for which it was designed. The phase transformation of δ-Cr occurs in the temperature range of the heat treatments of many steels and metallic alloys, as for instance Zircaloy-4 used in nuclear industry which will lose its metallurgical state as cladding material above 753 K [37]. If a Cr coating is deposited by DLI-MOCVD on this alloy, the disappearance of the metastable phase δ-Cr will reveal incidental conditions in service greater than 723 K which will also affect the properties of the zirconium alloy. Obviously, the exposure time also plays an important role in this δ-Cr/α-Cr transformation, but a kinetic study of this transformation was not the primary purpose of this paper and it will be investigated shortly.

Preliminary results of mechanical properties were obtained using a nanoindenter (Nano scratch tester, CSM instrument) for monolayer and multilayer coatings deposited on steel at 673 K using C_6H_5SH as inhibitor. The data are reported in Table S1 (Supplementary material) and are compared to previous values for similar coatings. The nanohardness of a columnar 3.5 μm thick monolayer coating is 9.7 GPa. This is consistent with the 13.0 GPa found for columnar monolayer coatings deposited at the same temperature with C_6Cl_6 as inhibitor [18]. More interesting for technological application is the higher nanohardness of 16.9 GPa found for a 5.5 μm thick multilayer coating that exhibits a high density (deposited according mode 2). When Cr coatings grown by MOCVD and DLI-MOCVD using C_6Cl_6 as inhibitor are sufficiently dense, they also exhibit a comparable high nanohardness of 19.0 [18] and 17.0 GPa [22], respectively. Whatever the inhibitor used (C_6Cl_6 or C_6H_5SH) dense coatings have an elastic modulus in the range 270–310 GPa which is close to the 285 GPa of bulk Cr. Furthermore they all exhibit a compressive residual stress close to 0.6 GPa (determined from the curvature change of samples).

We will no longer comment on these preliminary properties, but there are two strengths that must be retained: *(i)* DLI-MOCVD Cr metal coatings are much harder than those deposited by other techniques, *e.g.* electrodeposition [1–3] or arc evaporation [8], and *(ii)* there is no significant difference for MOCVD and DLI-MOCVD coatings depending on the nature of the inhibitor used, which means that the presence of the metastable phase δ-Cr does not significantly affect mechanical properties. The very high hardness of the same order of magnitude as that of chromium carbides is probably due to carbon supersaturation in Cr as revealed by XPS analyses (Fig. 7). The fact that the metastable phase would not affect the mechanical properties of the two-phase coatings would be due to the cubic structure of each component, their very similar density and the small amount of δ-Cr.

4. Conclusions

A low amount (<6%) of the cubic metastable δ-Cr phase was found mixed with the stable bcc-Cr phase in DLI-MOCVD coatings. The formation of this metastable phase results from both the low temperature of deposition (<723 K) and the use of thiophenol as inhibitor of carbide formation. It was not reported under other CVD conditions. Dense coatings were deposited by implementing a multilayer growth mode in order to avoid a columnar and porous morphology. Such coatings exhibit a high nanohardness of about 17 GPa.

According to the literature, this metastable phase is irreversibly transformed into the stable bcc one from 723 K in inert atmosphere. This structural transformation should not affect the properties of the coating due to the similarity of their crystallographic structures (both cubic) and their very close density (a volume contraction of only 0.4% at the time of structural transformation). The presence of this metastable phase constitutes a signature of the DLI-MOCVD process. It can be used as a tracer for coatings operating in high temperature environment without loss of the basic properties of the coatings. This is particularly useful in non-destructive testing of manufactured structural components.

Acknowledgements

The authors thank Dr. Arnaud Proietti and Marie-Christine Lafont for their help in EBSD and TEM analyses respectively, and R. Laloo for nanohardness measurement. RBS analyses were made by H. Guégan in ARCANE-CENBG, Gradignan, France. This work was partially supported by CNRS, CEA, INPT and the Centre of Excellence of Multifunctional Architectured Materials (CEMAM).

Appendix A. Supplementary data

Supplementary data associated with this article can be found, in the online version, at doi: 10.1016/j.apsusc.2017.05.253.

References

[1] S. Hoshino, H.A. Laitinen, G.B. Hoflund, The electrodeposition and properties of amorphous chromium films prepared from chromic acid solutions, J. Electrochem. Soc. 133 (1986) 681–685.
[2] N. Imaz, M. Ostra, M. Vidal, J.A. Díez, M. Sarret, E. García-Lecina, Corrosion behaviour of chromium coatings obtained by direct and reverse pulse plating electrodeposition in NaCl aqueous solution, Corros. Sci. 78 (2014) 251–259.
[3] G.A. Lausmann, Electrolytically deposited hardchrome, Surf. Coat. Technol. 86–87 (Part 2) (1996) 814–820.
[4] A. Liang, L. Ni, Q. Liu, J. Zhang, Structure characterization and tribological properties of thick chromium coating electrodeposited from a Cr(III) electrolyte, Surf. Coat. Technol. 218 (2013) 23–29.
[5] V.S. Protsenko, F.I. Danilov, V.O. Gordiienko, A.S. Baskevich, V.V. Artemchuk, Improving hardness and tribological characteristics of nanocrystalline Cr-C films obtained from Cr(III) plating bath using pulsed electrodeposition, Int. J. Refract. Met. Hard Mater. 31 (2012) 281–283.
[6] A. Aubert, R. Gillet, A. Gaucher, J.P. Terrat, Hard chrome coatings deposited by physical vapour deposition, Thin Solid Films 108 (1983) 165–172.
[7] F. Cosset, G. Contoux, A. Celerier, J. Machet, Deposition of corrosion-resistant chromium and nitrogen-doped chromium coatings by cathodic magnetron sputtering, Surf. Coat. Technol. 79 (1996) 25–34.
[8] G. Cholvy, J.L. Derep, M. Gantois, Characterization and wear resistance of coatings in the Cr-C-N ternary system deposited by physical vapour deposition, Thin Solid Films 126 (1985) 51–60.
[9] S. Komiya, S. Ono, N. Umezu, Hardness and grain size relations for thick chromium films deposited by hallow cathode discharge, Thin Solid Films 45 (1977) 473–479.
[10] H. Högberg, L. Tengdelius, M. Samuelsson, J. Jensen, L. Hultman, β-Ta and α-Cr thin films deposited by high power impulse magnetron sputtering and direct current magnetron sputtering in hydrogen containing plasmas, Phys. B: Condens. Matter 439 (2014) 3–8.
[11] R.G.I. Leferink, W.M.M. Huijbregts, Chromium diffusion coatings for the protection of low-alloy steel in a sulphidizing atmosphere, Corros. Sci. 35 (1993) 1235–1242.
[12] V.A. Ravi, Pack cementation coatings, in: S.D. Cramer, B.S. Covino Jr. (Eds.), ASM Handbook Volume 13A: Corrosion: Fundamentals, Testing, and Protection, ASM International, 2003, 2017, pp. 763–771.
[13] A.R. Castle, D.R. Gabe, Chromium diffusion coatings, Int. Mater. Rev. 44 (1999) 37–58.
[14] F. Maury, L. Gueroudji, C. Vahlas, Selection of metalorganic precursors for MOCVD of metallurgical coatings: application to Cr-based coatings, Surf. Coat. Technol. 86–87 (Part 1) (1996) 316–324.
[15] A. Michau, F. Maury, F. Schuster, R. Boichot, M. Pons, E. Monsifrot, Chromium Carbide Growth at Low Temperature by a Highly Efficient DLI-MOCVD Process in Effluent Recycling Mode, Surf. Coat. Technol. (2017), submitted for publication.
[16] F. Maury, F. Ossola, Evaluation of tetra-alkylchromium precursors for organometallic chemical vapor deposition I: Films grown using $Cr[CH_2C(CH_3)_3]_4$, Thin Solid Films 207 (1992) 82–89.
[17] V.B. Polikarpov, A.S. Luzin, V.A. Dodonov, E.K. Klement, Chromium films obtained by pyrolysis of chromium bisarene complexes in the presence of chlorinated hydrocarbons, Izvestiya Akademii Nauk SSSR 20 (1984) 1839–1842.
[18] F. Maury, C. Vahlas, S. Abisset, L. Gueroudji, Low temperature metallorganic Chemical Vapor Deposition routes to chromium metal thin films using bis(benzene)chromium, J. Electrochem. Soc. 146 (1999) 3716–3723.
[19] F. Maury, F.-D. Duminica, F. Senocq, Novel MOCVD process for the low temperature deposition of the chromium nitride phases, in: M.D. Allendorf, M.L. Hitchman (Eds.), CVD XV: Proceedings of the Fifteenth International Symposium on Chemical Vapor Deposition, The Electrochemical Society, Pennington, NJ, 2000, pp. 260–267.
[20] C. Vahlas, F. Maury, L. Gueroudji, A thermodynamic approach to the CVD of chromium and of chromium carbides starting from $Cr(C_6H_6)_2$, Chem. Vap. Depos. 4 (1998) 69–76.
[21] A.S. Luzin, V.B. Polikarpov, V.A. Dodonov, E.K. Klement, Chromium films obtained by pyrolysis of bis(arene)chromium complexes in presence of sulfur-containing additives, Zh. Prikl. Khim. 61 (1988) 1235–1239.
[22] F. Maury, A. Douard, S. Delclos, D. Samelor, C. Tendero, Multilayer chromium based coatings grown by atmospheric pressure direct liquid injection CVD, Surf. Coat. Technol. 204 (2009) 983–987.
[23] A. Douard, C. Bernard, F. Maury, Thermodynamic simulation of atmospheric DLI-CVD processes for the growth of chromium-based hard coatings using bis(benzene)chromium as molecular source, Surf. Coat. Technol. 203 (2008) 516–520.
[24] G. Boisselier, F. Maury, F. Schuster, Growth of chromium carbide in a hot wall DLICVD reactor, J. Nanosci. Nanotechnol. 11 (2011) 8289–8293.
[25] K. Kimoto, I. Nishida, An electron diffraction study on the crystal structure of a new modification of chromium, J. Phys. Soc. Jpn. 22 (1967) 744–756.
[26] I. Nishida, K. Kimoto, Crystal habit and crystal structure of fine chromium particles: an electron microscope and electron diffraction study of fine metallic particles prepared by evaporation in argon at low pressures (III), Thin Solid Films 23 (1974) 179–189.
[27] J. Forssell, B. Persson, Growth and structure of thin chromium films condensed on ultra-high vacuum cleaved NaCl and KCl crystals, J. Phys. Soc. Jpn. 29 (1970) 1532–1545.
[28] J. Reyes-Gasga, G.R. Garcia, M. Jose-Yacaman, Electron-beam-induced structure transformation of the quasicrystalline phases of the $Al_{62}Cu_{20}Co_{15}Si_3$ alloy, Radiat. Phys. Chem. 45 (1995) 283–291.
[29] K. Yin, Y. Xia, Z. Liu, J. Yin, L. Sun, Electron-beam induced phase transformation in β-Ag_2Se thin films, Phys. Status Solidi (a) 209 (2012) 135–138.
[30] U. Golla-Schindler, G. Benner, A. Orchowski, U. Kaiser, In situ observation of electron beam-induced phase transformation of $CaCO_3$ to CaO via ELNES at low electron beam energies, Microsc. Microanal. 20 (2014) 715–722.
[31] W.D. Klopp, Recent developments in chromium and chromium alloys, JOM 21 (1969) 23–32.
[32] J. Oudar, N. Barbouth, Solubility of sulphur in iron-chromium alloys, Scr. Metall. 15 (1981) 41–43.
[33] A. Michau, F. Maury, F. Schuster, I. Nuta, R. Boichot, M. Pons, Chromium carbide growth by direct liquid injection chemical vapor deposition in long and narrow tubes, experiments, modeling and simulation, submitted for publication.
[34] R.G. Hennig, D.R. Trinkle, J. Bouchet, S.G. Srinivasan, R.C. Albers, J.W. Wilkins, Impurities block the [alpha] to [omega] martensitic transformation in titanium, Nat. Mater. 4 (2005) 129–133.
[35] R.S. Fishman, S.H. Liu, Effect of impurities on the magnetic ordering in chromium, Phys. Rev. B 45 (1992) 12306–12318.
[36] D.A.H. Hanaor, C.C. Sorrell, Review of the anatase to rutile phase transformation, J. Mater. Sci. 46 (2011) 855–874.
[37] S. Fourgeaud, J. Desquines, M. Petit, C. Getrey, G. Sert, Mechanical characteristics of fuel rod claddings in transport conditions, Packag. Transp. Storage Secur. Radioact. Mater. 20 (2009) 69–76.